Hydrothermal carbonization of olive wastes to produce renewable, binder-free pellets for use as metallurgical reducing agents

Gerrit Ralf Surup[a], James J. Leahy[b], Michael T Timko[c], Anna Trubetskaya[b,*]

[a]*Department of Materials Science and Engineering, Norwegian University of Science and Technology, 7491, Trondheim, Norway*
[b]*Bernal Center, University of Limerick, Castletroy, Ireland*
[c]*Chemical Engineering Department, Worcester Polytechnic Institute, 01609 Worcester, MA, USA*

Abstract

Torrefaction or hydrothermal carbonization processes were compared for conversion of olive pulp into metallurgical reducing agent. The dependence of yield, CO_2 reactivity, and mechanical properties to reaction time and heat treatment temperature was investigated. Hydrochar yield increased with increasing residence time and the maximum solid yield was observed for a residence time of 15 h. On the other hand, CO_2 reactivity slightly decreased with increasing heat treatment temperature at a residence time of 2 h. Notably, the CO_2 reactivity of hydrochar was less than that of olive pulp char produced by torrefaction, approximating that of carbon-based reducing agents derived from non-renewable resources. An additional heat treatment improved hydrochar pellet durability to greater than 95 %, whereas stable torrefied char pellets could not be produced under any set of conditions. Hydrothermal

*Corresponding author email: anna.trubetskaya@ul.ie

carbonization is superior to torrefaction for production of renewable reducing agents with reactivity and mechanical properties comparable to those afforded by reducing agents from non-renewable sources.

---

1. Introduction

Metallurgical conversion of oxides to their base metals is responsible for about 10 % of all CO_2 emissions worldwide [1, 2]. Similar to replacement of petroleum with biofuels, replacement of fossil fuel-derived reducing agents with renewable versions derived from waste biomass can reduce metal processing emission. In addition to CO_2 emissions reductions, replacing fossil-based coke with biochar can improve off-gas quality by decreasing the SO_x and NO_x emissions from the steel and ferroalloy industries [3–9]. Current metallurgical production relies on fossil-based materials because the use of biomass-ore pellets in the reduction process can increase the overall power consumption by 72-152 kWh per tonne of FeMn, thereby increasing processing costs [10]. However, optimizing biochar's material properties to improve its electrical conductivity and retain acceptable reactivity might reduce total production cost [11]. The challenge then is identification of low cost biomass sources and energy and cost efficient methods for converting these biomass sources into effective reducing agents [12].

Regional differences in biomass availability [12] translate into differences in metallurgical practice. Ireland is one of the least forested countries in Europe with less than 10.5 % of its land occupied by forest ($\approx$ 697,600 ha),

2

and accordingly Ireland relies on fossil derived materials for metallurgical purposes. In comparison, Sweden and Norway are heavily forested and rely on woodchips and pelletized wood for energy and metallurgical purposes [13, 14].

Making more widespread use of biomass-derived reducing agents is required so that the emissions reduction benefits can be spread to regions that lack natural forestry resources. Limiting agricultural and food waste has become a major concern throughout the world; within the EU, approximately 700 million tons of agricultural wastes are generated annually, which is expected to increase by 70 % by 2025 [15, 16]. In particular, agricultural residues generated in the Mediterranean region represent a major biomass source, especially from production of olive oil. In fact, the Mediterranean countries are responsible for over 98 % of worldwide oil production, and a similar percentage of the associated waste [17].

The most important properties of carbonaceous reductant are low cost, low reactivity, and low levels of impurities [18]. Low cost can be achieved by use of low-cost feeds (such as olive waste) and efficient processes to convert these wastes into usable forms. Low ash content is an important property because each additional percent of ash can increase slag volume by about 10-15 kg t^{-1} of ferroalloy, thereby increasing the electric power required for smelting [19]. Unfortunately, most biomass feeds cannot meet these stringent requirements, which necessitates identification of effective processes for upgrading inexpensive feeds into a form that can be useful for metallurgy. Hydrothermal carbonization (HTC) and pyrolytic torrefaction have promise for converting raw biomass into useful forms at modest temperatures (<

3

250°C). In fact, both of these processes show potential for producing carbon-rich solids for hydrogen storage, electrochemical energy storage, water purification, or use in the gasification and metallurgical industries [20–23]. HTC is carried out in a hot liquid water in the temperature range 180 to 250°C at solids loading ranging from 7 to 25 %, and reaction time ranging from a few minutes to several hours [24]. Torrefaction is a mild pyrolysis process that converts biomass into a more carbon-rich material with increased energy density and decreased oxygen content. Consistent with current usage, the product of HTC can be termed "hydrochar", while the product of torrefaction can be termed "biochar" [23, 25]. "Char" will be used as a general term that encompasses both hydrochar and biochar. Previous work suggests that hydrothermal carbonization produces a material with superior metallurgical properties compared with torrefaction biochar [26]. Specifically, HTC removes a significant fraction of undesired inorganic elements such as Na and K that would otherwise contribute to slag [27]. Previous studies showed that the alkali content can be further reduced by increasing the heat treatment temperature or by washing the hydrochar with the deionized water after the pretreatment [28–34]. The use of a reductant with low alkali content can decrease the reactivity and thus, reduce the maintenance costs due to the increased electrical conductivity [35, 36]. In opposite, the ash content of feedstock is known to change only slightly during torrefaction in the distribution of calcium, magnesium, and manganese, with some change in water soluble potassium [37–41]. Therefore, based on the literature alone the fate of interaction of alkali metals with the carbonaceous matrix of hydrochar and biochar during ferroalloy reduction is not clear. The mechanical properties

4

of chars are also important for many applications, including metallurgical ones. Torrefied biomass particles are loose and nonuniform due to decreased hemicellulose content [42]. In comparison, hydrochar has superior mechanical strength and pelletability compared with torrefaction biochar [27, 43, 44]. Beside the complexity of structure-property relationship, the use of bioductants is hindered by the price of feedstock and hydrochar yield [45, 46]. Sensitivity analysis indicates that this breakeven selling price could be as low as 106 US dollars per ton, depending on the capacity of the plant [47]. Feedstock costs and char yield influence this estimate [25, 47]. Pretreatment of raw feedstock, e.g. supercritical CO_2 extraction, has potential to improve properties without negatively impacting char yield [48, 49].

No general theory can currently predict which of these two methods, HTC or torrefaction, is most suitable for converting a given feedstock into a metallurgical reducing agent. Literature data is scarce that describes the effect of residence time and temperature on resulting hydrochar or biochar properties that impact metallurgical applications, adding uncertainty to the use of hydrochar or biochar as a reducing agent. A particular challenge is tuning conditions to maximize yield while producing a solid with acceptable reactivity, conductivity, and mechanical properties. In this study, the impact of heat treatment temperature, residence time on char yield and properties obtained by of the HTC carbonization and torrefaction of olive waste was investigated. The specific objectives of this study were to: (1) compare the yields obtained from the HTC and torrefaction processes, (2) understand the influence of heat treatment temperature and residence time on the char properties and (3) develop structure-property relationships governing the CO_2

5

reactivity and electrical resistance of pellets made from hydrochar.

2. Materials and Methods

Olive pulp from Tunisia was obtained as a feedstock for this study. Fuel selection was based on its high bulk density and abundance. Hydrochar samples were generated by placing olive pulp in a closed stirred batch reactor heated to a temperature in the range from 190 to 250°C with a residence time of 2, 6 or 15 h. Torrefaction was performed in a thermogravimetric analyzer. Pellets were made by pressing the olive pulp char without binder. Char powder and pellet properties were evaluated using scanning electron microscopy, thermogravimetric analyzer, Bunsen burner, high-temperature dielectric four-probe system, Fourier-transform infrared spectroscopy, and bomb calorimetry. Error bars represent standard deviation from the mean of the series of measurements. All measurements were conducted in triplicate to establish sufficient reproducibility within $< 2\%$.

2.1. Hydrothermal carbonization

HTC experiments were performed in a stirred batch reactor (1 L Series 4520 bench top reactor, Parr Instrument Company, USA) equipped with an external resistance heater and internal sensors for pressure and temperature measurement. The pressurized vessel (inner diameter: 100 mm, height: 135 mm) was made of stainless steel. A safety pressure of 62 bar was set using a burst disc. The pressure and temperature were recorded continuously at 1 s intervals. Before each experiment, 120 g of olive pulp and 380 g of deionized water were placed in the reactor and the reactor was sealed. The sample was

heated to a final temperature ranging from 190 to 250°C at a heating rate of 5°C min^{-1} and kept at the final temperature for reaction times varying between 2 and 15 h, depending on temperature. The sample was homogenized using an anchor-shaped agitator at a constant speed of 90 rpm during the experiment.

After reaching the desired reaction time, the external heater was removed and replaced with a water reservoir to cool to less than 100°C. When the temperature fell below 50°C, the stirrer was turned off and the gas was released into a gas sampling bag. CO_2 and CH_4 gas concentrations were analyzed using a SSM6000 biogas analyzer (Pronova, Germany). The slurry was filtered and the solid residue was dried 113 at 105°C. The dried samples were stored in sealed plastic containers.

2.2. Torrefaction

Torrefaction of olive pulp was performed in a thermogravimetric instrument TGA/DSC 1 STARe System (Mettler Toledo, USA). For each experiment, 50 mg of crushed olive pulp sample were loaded into a 150 μl Al_2O_3 crucible. The sample was heated at 25 °C min^{-1} to a pre-determined final temperature and kept at that temperature for 2, 6 or 15 hours, similar to the reaction times examined for hydrothermal carbonization. The system was continuously purged with nitrogen at a defined flow rate of 100 ml min^{-1} until the heating program was finished. The sample was then cooled to room temperature and stored in a sealed sample container.

7

2.3. Bunsen burner

The swelling index of hydrochar samples was analyzed using a Bunsen burner following a well known procedure [50]. For these tests, 1 g of crushed olive pulp hydrochar was weighed into a quartz glass crucible, closed with a quartz lid, and heated to 820°C within 150 s using a Bunsen burner with an inner diameter of 100 mm. After the sample was cooled to room temperature, the shape of the sample surface was compared to standard profiles and assigned to a number between 0 and 9. Each experiment was carried out in duplicate.

2.4. Char characterization

Carbon content analysis. The carbon content of the liquid sample obtained after HTC was analyzed using a TOC Analyzer 5050A (Shimadzu Scientific Instruments, USA).

Elemental analysis. Elemental analysis was performed on feed materials and char products using an Analyzer Series II (Perkin Elmer, USA). Acetanilide was used as a reference standard. The ash content was determined using a standard ash test at 550°C, according to the procedure described in DIN EN 14775.

Swelling index. The swelling index of hydrochars was investigated following the procedure described in DIN EN 51741.

Calorific value. The calorific value was determined by bomb calorimetry C200 (IKA, Germany), according to the procedure described in ISO 1928.

Scanning electron microscopy. SEM analysis of char samples was conducted using a high-resolution field emission microscope JSM-7800F (JEOL, Japan). Prior to analysis, char samples were coated with a thin layer of gold (2 min, 20 mA) using an Edwards S150B Sputter Coater to avoid sample charging.

Thermogravimetric analysis. The reactivity of low temperature char and hydrochar was analyzed by exposing samples to a reactive gas consisting of either CO_2 or air in a thermogravimetric instrument TGA/DSC 1 System. For each experiment, 5 mg of milled sample were loaded into an alumina crucible. The samples were heated at a constant heating rate of $10°C$ min^{-1} to $110°C$ and kept for 15 min for drying. The dried sample was subsequently heated to $1100°C$ at a constant heating rate of $10°C$ min^{-1}. In addition, the thermal properties of hydrochar samples was investigated under inert gas consisting entirely of Ar.

Pellet press. Prior to pelletization, 1.2 g of hydrochar was homogenized with 1 g of water as a binding agent. A compact hot pellet press (MLI, USA) was used for pelletization. The hot pellet press consisted of a metal cylinder with a press channel and a backstop. The pellet diameter was 6.5 mm, formed by application of 1 kN. Three separate pellets were pressed for each hydrochar.

Mechanical durability. The mechanical durability of hydrocharpellets was investigated using an ISO tumbler 1000+ (Bioenergy, Austria) in accordance with ISO 17831-1. Single pellets were rotated for 10 min at 50 rpm and the pellet recovered and separated from lose powder formed during tumbling. The mechanical durability was estimated as the ratio of final pellet mass to its initial value.

FTIR Spectroscopy. The hydrochar samples were analyzed using a Cary 630 FTIR spectrometer (Agilent, USA) equipped with an attenuated total reflectance (ATR) attachment. All absorption spectra were obtained in the 4000-600 cm^{-1} range by 100 scans at 4 cm^{-1} resolution. For background, 200 scans were acquired. All samples were measured in triplicate and average spectra are provided here.

Electrical resistivity. Electrical conductivity measurements were performed using a 34470A 7 1/2 Digit Multimeter (Keysight Technologies, USA). The cell geometry was the same as recommended by Sun et al. [51] and the analysis method was that recommended by van der Pauw et al. [52]. The electrical conductivity was determined according to equation 1:

$$\sigma = \frac{L}{R \cdot A} \tag{1}$$

In equation 1, σ is the electrical conductivity, A is the cross-sectional areaof the sample, L is the length of the resistor, and R is the known resistance between the Ti-Au electrodes.

3. Results and discussion

3.1. Original feedstock characterization

Table 1 provides compositional data obtained from analysis of the olive pulp feed. As expected, olive pulp consists primarily of carbon and oxygen, with a HHV similar to other biomass types [53]. The ash content of olive pulp was less than that of olive stones, whereas olive pulp contained more calcium than olive stones [25].

10

Table 1: Proximate, ultimate and ash analyses of olive pulp.

Biomass	Proximate analysis				Ultimate analysis					HHV
	MC	VM	FC	ash	C	H	N	S	O	
	%, ar		%, db				%, db			MJ kg^{-1}
	10.0	72.0	24.2	3.8	44.6	6.1	1.1	0.1	44.3	16.7
Olive pulp	Ash compositional analysis (mg kg^{-1} on dry basis)									
	Cl	Al	Ca	Fe	K	Mg	Na	P	Si	Ti
	0.01	100	1650	70	1600	150	300	100	1800	10

3.2. Product yields

Figure 1 provides product yields obtained from the HTC of olive pulp as solids (char), liquids (both aqueous and organic fractions), and major gases. The liquid yield was measured by total organic carbon (TOC) analysis, whereas the gas yield was determined using the total gas volume and concentrations of CH_4 and CO_2. The hydrochar yield decreased from 61 to 35 % when temperature was increased over the range from 190 to 250°C and residence time at a constant reaction time of 6 h, consistent with previous observations [54].

Hydrochar yields of 65.3, 60.4 and 51.6 % were measured at 200, 220 and 240°C with 2 h residence time, similar to yields reported for HTC of olive pomace [55]. Hydrochar yields obtained after 30 min residence time were 10 % greater than those obtined at 2 h, emphasizing the effect of residence time on the hydrochar yield for olive pulp [43, 55]. In contrast, hydrochar yields obtained from corn-cob are nearly insensitive to residence time, stressing the importance of feedstock properties on the conditions which optimize

11

hydrochar yield [56].
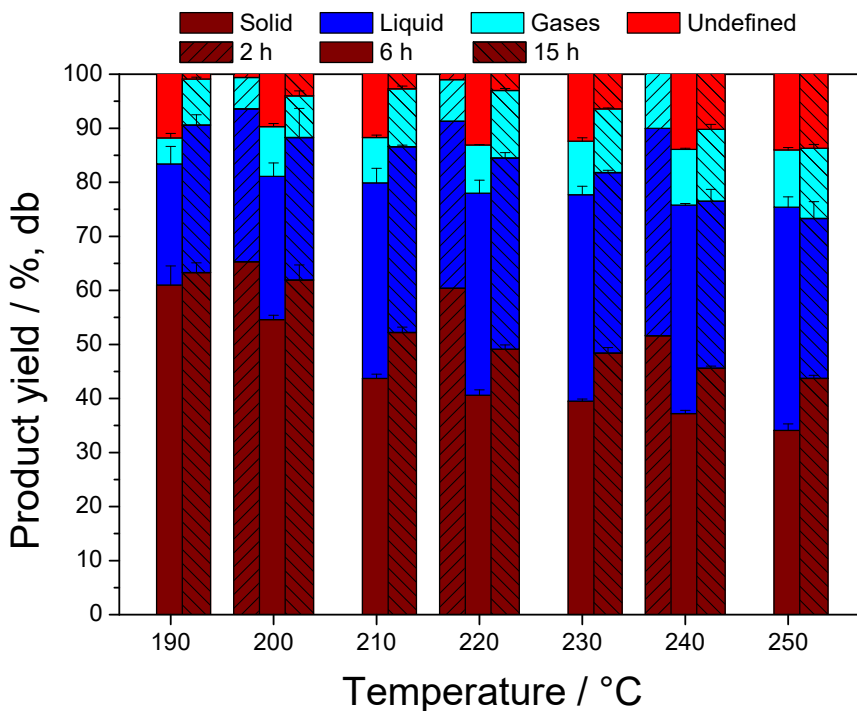

Figure 1: Yields of hydrochar, liquid and gaseous products.

Increasing the residence time to 15 h increased hydrochar yield by about 8 %, an observation attributable to formation of secondary char by polymerization reactions of small molecules in the liquid phase and recondensation into the char phase [38]. Secondary char forming reactions from dissolved organic material have been reported to increase hydrochar yield by 5-10 % [43, 57–59]. Secondary char forming reactions produce a sphere-like structure with overlapping layers and greater carbon content than the primary char [43]. Increasing HTC temperature first increases hemicellulose solubility and hydrolysis rates, then promotes structural changes in cellulose

12

and lignin, finally results in a lower hydrochar yield, consistent with previous results reported by Yang et al. [60].

3.3. Proximate analysis

Figure 2 shows results from the proximate analysis of hydrochar samples. The fixed carbon content increased from 32 to 43 % over the temperature range from 200 to 240°C at 2 h residence time. Similarly, increasing the reaction time increased the fixed carbon content, presumably the result of decarboxylation reactions that occurred during treatment and possibly re-combination reactions which result in a solid with greater fixed carbon than either the feed or the primary char. The fixed carbon content produced after 15 h HTC treatment was nearly twice that reported values for 5 min HTC treatment and up to 20 % greater compared with HTC treatment for 30 min [43, 61]. The ash content of olive pulp hydrochar remained nearly constant with treatment conditions, indicating that even the shortest, mildest HTC treatment achieved the same solubilization of minerals as longer, more intense treatments. In contrast, previous studies reported that HTC significantly decreases ash content and residual alkali metals contained with hydrochar, leading to increased reactivity of hydrochar product [54, 55]. This suggests that the mineral content of olive pulp may be more thermally stable and water insoluble than other biomass types.
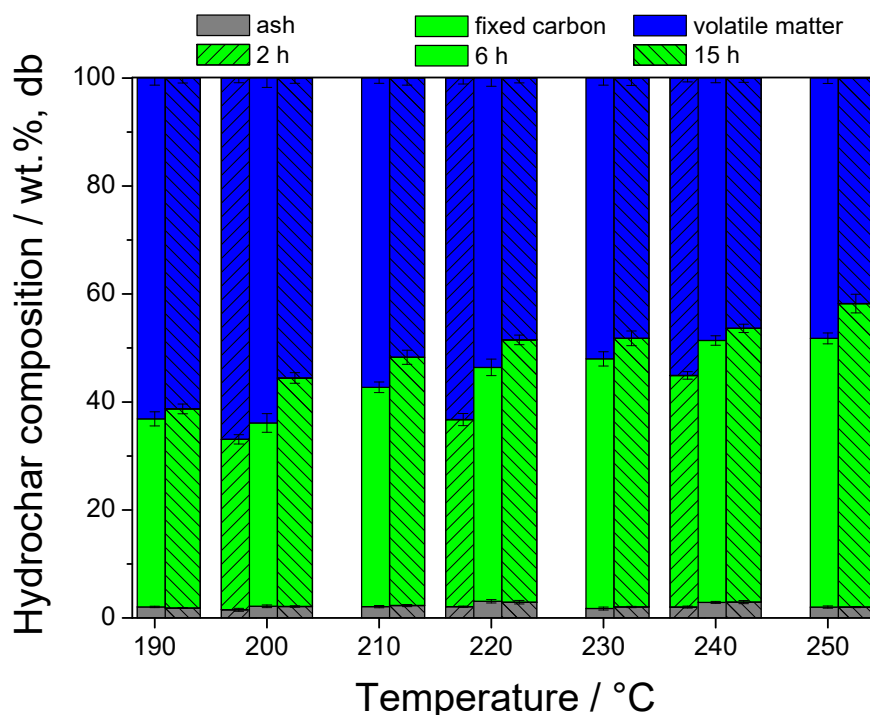
Figure 2: Proximate analysis of hydrochar samples.

3.4. Elemental analysis

Figure 3 shows a van Krevelen plot of the compositions of olive pulp and hydrochar samples. The original composition data are summarized in the supplemental material (Table-S1). Figure 3 shows that the hydrogen and oxygen content decreased with increasing HTC temperature, the result of both dehydration and decarboxylation reactions. For example, for a constant 2 h HTC treatment time, the carbon content increased from 57.7 to 67.7 % over the temperature range 200 to 240 °C, consistent with previous results reported by Volpe and Fiori [43].

14
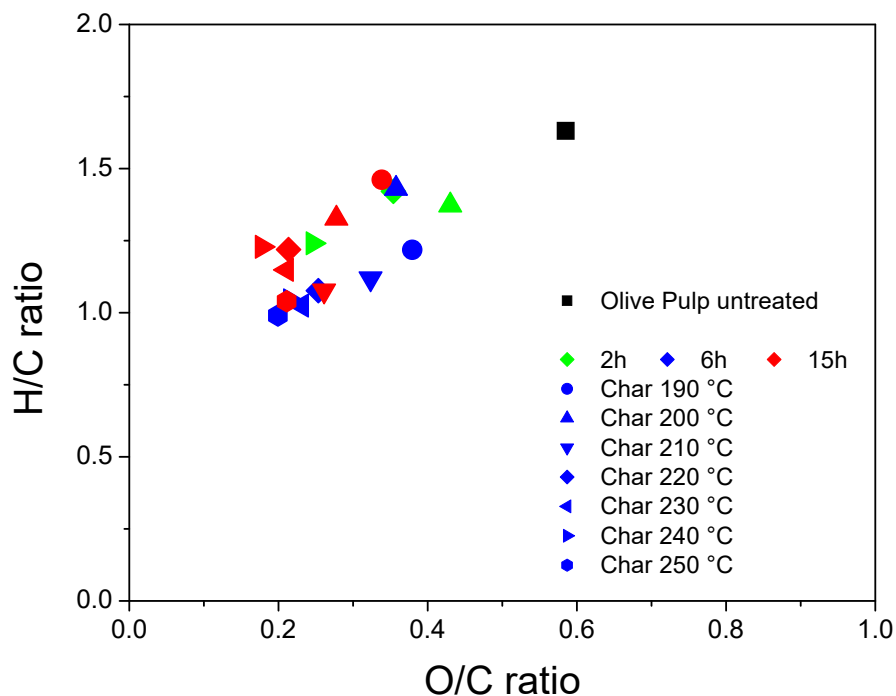
Figure 3: Van Krevelen diagram of hydrochar samples.

3.5. Calorific value

Figure 4 shows the heating values measured for hydrochar samples. As expected from Figure 3, the heating value increased with increasing heat treatment temperature and increasing residence time. The heating value of olive waste pulp was increased from 16.7 to 29.5 MJ kg^{-1} for the hydrochar prepared at 250°C. This value is similar to the heating value of hydrochar generated from wood and straw and approaches that of hard coal [43, 62, 63]. Feedstock selection apparently has only a minor effect on the heating value of hydrochar compared with the significant effect of heat treatment temperature and residence time.

15
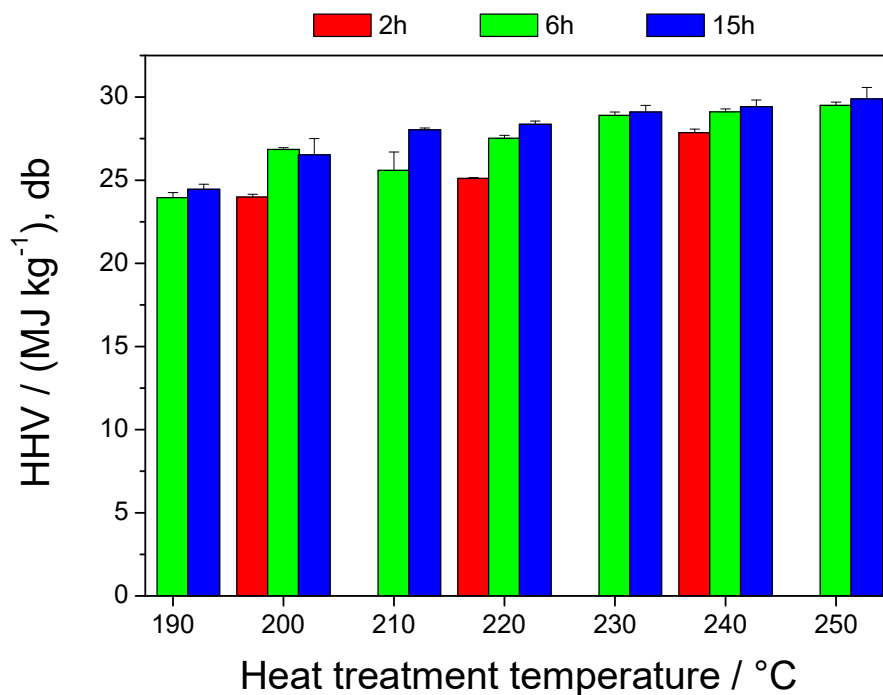
Figure 4: Calorific values of hydrochar samples.

3.6. Reactivity

Figure 5 shows differential weight loss curves (DTG) obtained by heating olive pulp, hydrochar, and biochar in argon or CO_2 environments. More information on the biochar is provided in Figure S-2-S-3. Thermal decomposition of olive pulp occurred over the temperature range from 200 to 600°C with a peak temperature of 320°C. In contrast, initial mass loss of hydrochar samples occurred at 150°C, with a peak temperature of 335°C. The initial mass loss of hydrochar samples is attributed to volatilization of hydrocarbons which are not directly incorporated in the solid matrix.
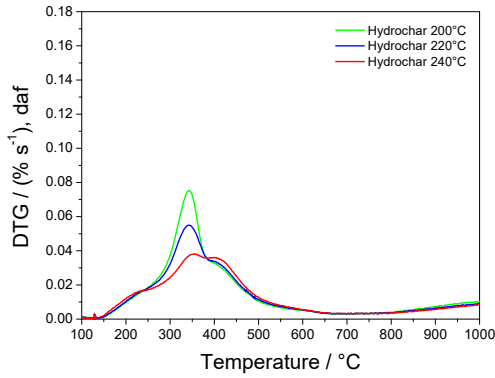
5(a): Torrefaction, 2 h
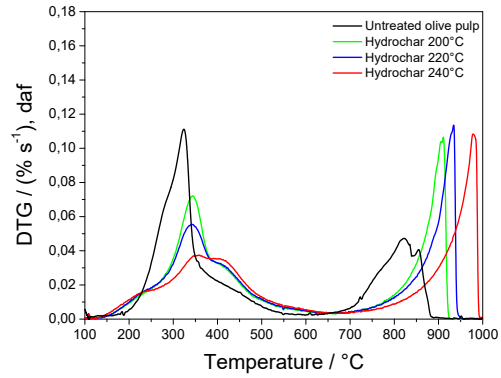
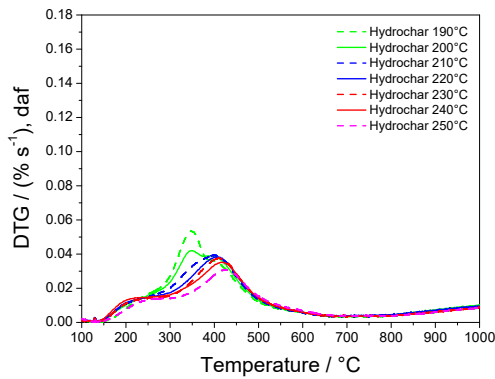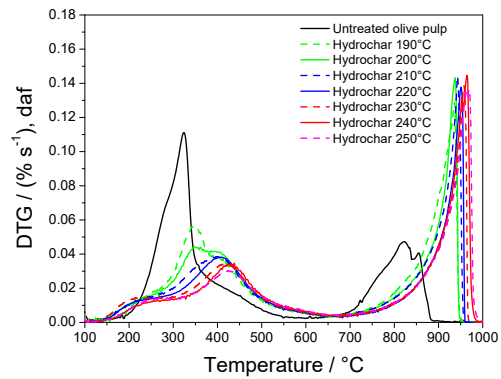5(b): 100 % CO$_2$, 2 h
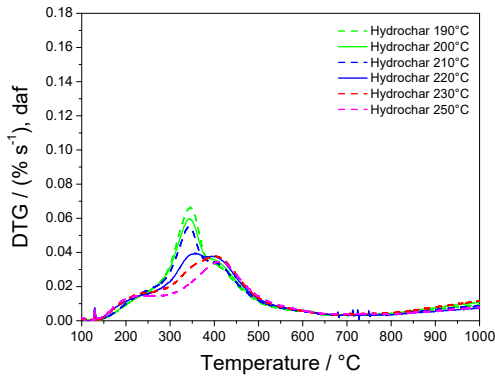
5(c): Torrefaction, 6 h
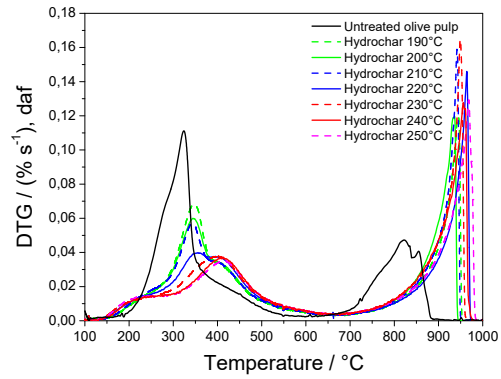
5(d): 100 % CO$_2$, 6 h

5(e): Torrefaction, 15 h

5(f): 100 %, CO$_2$, 15 h

Figure 5: DTG curves of olive pulp prepared at 190, 220 and 240°C using hydrothermal carbonization and torrefaction using 100 % argon and 100 % volume fraction CO$_2$ gasification: (a)-(b) 2 h, (c)-(d) 6 h and (e)-(f) 15 h.

The peak temperature of biochar increased from 845 to 870°C when the heat treatment temperature of char was increased from 200 to 240°C. Likewise, the peak temperature of hydrochar samples increased from 900 to 965°C after 2 h HTC treatment and was about 100°C greater than for the low temperature reacted char. However, the torrefaction time used to produce biochar did not have a strong influence on the CO_2 reactivity. Thus, the CO_2 reactivity of hydrochar is similar to wood charcoal obtained from pyrolysis at temperatures above 900°C [64, 65].

3.7. Surface structure

The microstructure of olive pulp and hydrochar produced at 200 and 240°C is shown in Figure 6. The olive pulp feed exhibited a surface structure with different grain sizes (Figure 6(a)) and olive shape particles with diameter in the range from 5 to 10 μm (Figure 6(b)). The olive shape microparticles disappeared after HTC, presumably revealing the underlying surface. The underlying biomass is referred to as hard biomass, whereas soft biomass is formed by sequential liquefaction and re-condensation [66]. HTC at 240°C produced a material with smooth surfaces (Figure 6(f)) consistent with ex-traction of Klason lignin from the biomass followed by to recombination reactions between lignin and holocellulose [67, 68]. Hydrochar obtained at less than 230°C is similar to its biomass feed, whereas its surface is typically smooth when prepared at 270°C [69]. Here, olive waste hydrochar presents smooth surfaces even when prepared at 240°C (6 h). Formation of smooth surfaces was enhanced by increasing HTC temperature and increasing the reaction time, again consistent with trends expected from redeposition of condensation products on the surface [66].
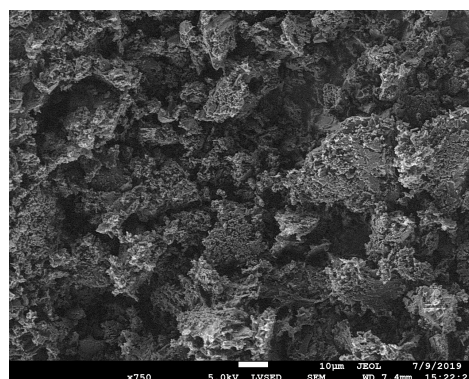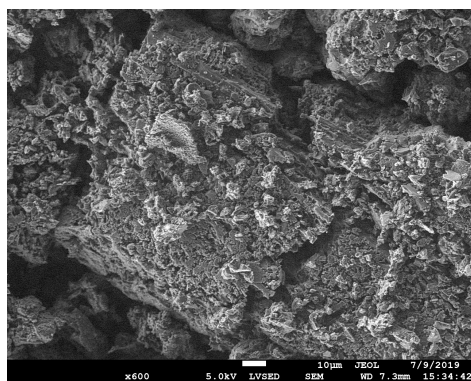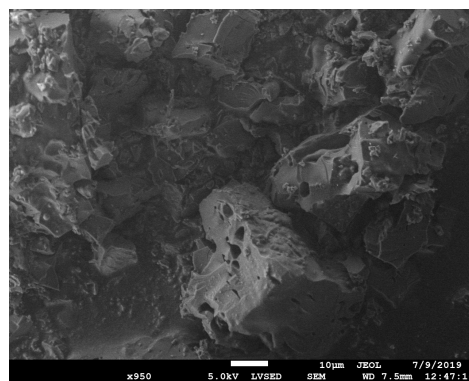
18
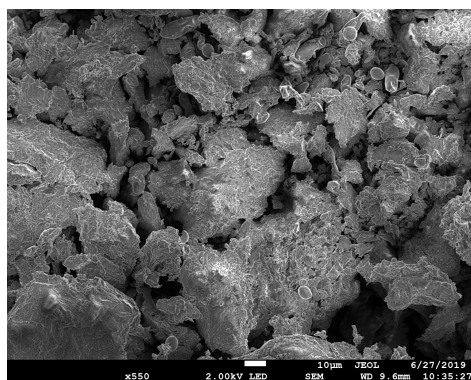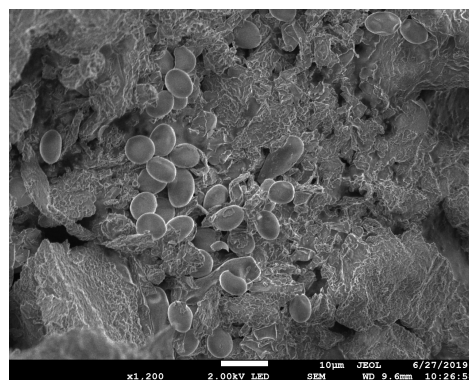
6(a): Olive pulp

6(b): Olive pulp
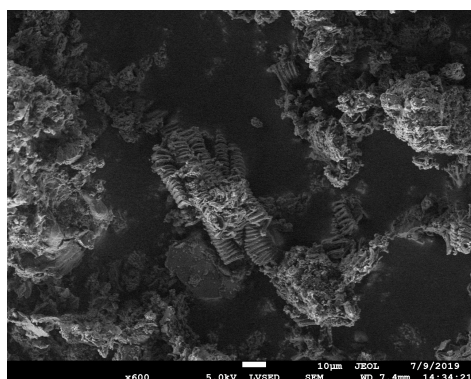
6(c): Hydrochar 200°C, 2h

6(d): Hydrochar 200°C, 15h

6(e): Hydrochar 240°C, 2h

6(f): Hydrochar 240°C, 15h

Figure 6: SEM image of (a)-(b) untreated olive pulp, and hydrochar produced at (c) 200°C, 2 h; (d) 200°C, 15 h; (e) 240°C, 2 h and (f) 240°C, 15 h.

19

3.8. FTIR

FTIR analysis was conducted to investigate the changes in main functional groups present in the hydrochar. Figure 7(a) provides olive pulp hydrochar spectra; spectral assignments are summarized in the supplemental material (Table S-2). The bands located between 3100 and 3700 cm^{-1} are associated with O-H vibration in hydroxyl or carboxyl groups which were found both in the original feedstock and hydrochar samples [70–73]. Strong vibration bands at 2855 and 2921 cm^{-1} originate with the aliphatic C-H stretching vibrations [59]. Differences between the untreated olive pulp and hydrochar mainly appeared in the spectral range 1020 to 1850 cm^{-1}. The major bands associated with the aromatic stretching and C=O stretch bands for all hydrochar samples were located at 1591 and 1700 cm^{-1} [59, 71, 73]. The band at 1636 cm^{-1} was present only in the hydrochar samples. The bands at 1442 and 1510 cm^{-1} were more intense in the hydrochar in the original olive pulp, indicating an increased aromaticity and possibly furanic content during the HTC treatment [59, 73]. Strong aromatic absorption bands of hydrochar samples indicated decomposition of olive pulp and re-polymerization of tar compounds [59]. IR analysis indicates that hydrochar is more aromatic than the original olive pulp, consistent with elemental composition data shown in Figure 3. Similarly, aromaticity increased in all hydrochar samples with the increasing heat treatment temperature.
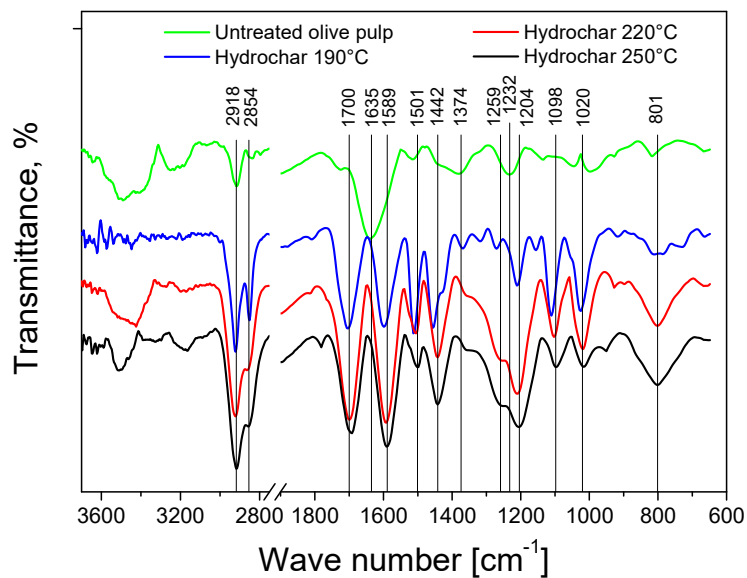
7(a): Temperature
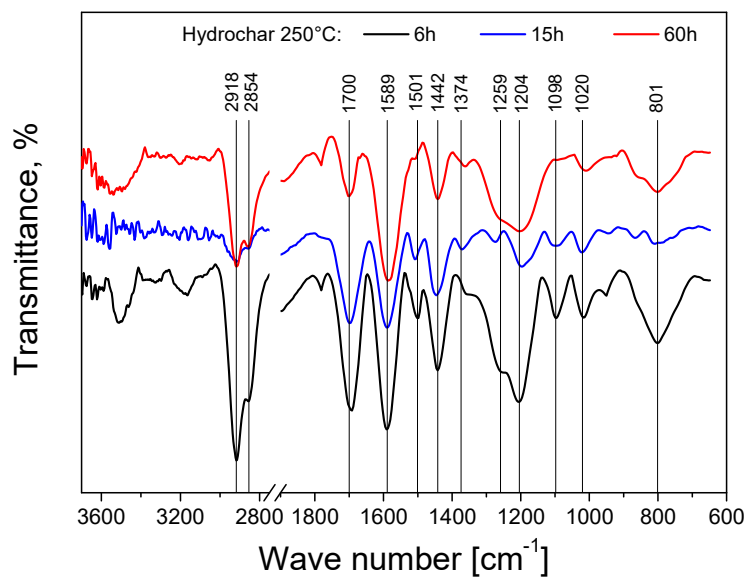
7(b): Residence time

Figure 7: Experimental IR spectra of (a) raw olive pulp and hydrochar produced at 190, 220 and 250°C with a residence time of 6 h; (b) olive pulp hydrochar generated at 250°C with a residence time of 6, 15 and 60 h.

21

The FTIR spectra of hydrochar produced at 250°C with residence times of 6, 15 and 60 h is shown in Figure 7(b). The bands located at 800 to 1800 cm^{-1} were present in all samples, but with different intensities. Hydrochar samples generated at 220 and 250°C showed similar band spectra, indicating that the main structural changes occur at temperatures less than 220°C. The bands at 1021 and 1099 cm^{-1} originate from C-O stretching vibration of hydrochar samples, whereas bands between 927 and 1127 cm^{-1} are assigned to C-O stretching vibration in cellulose and hemicellulose [74, 75]. The bands at 1206 and 1260 cm^{-1} were observed only for hydrochar samples produced at 220 and 250°C. This is probably due to the decomposition of hemicellulose at 220°C after 15 min hydrothermal treatment [24, 27]. The presence of the band and at 1206 cm^{-1} indicates increased ether content after HTC at 220 and 250°C. The C-O-C stretch intensity increased with the longer residence time, indicating the importance of etherification and/or esterification reactions during tar polymerization to form hydrochar.

3.9. Swelling index

Swelling properties are important for carbon reductants. The free swelling index (FSI) was 1.0-1.5 for all hydrochar samples, consistent with weak caking properties. Hydrochar samples produced in the temperature range 220 to 240°C exhibited a FSI of 1.5, whereas the FSI of all other hydrochar samples was 1.0. A swelling index of at least 2.5 is typically required for reductants [76], indicating that this property may need to be improved before the olive waste char is suitable for the ferroalloy industries [4]. However, previous results showed that gentle coking can improve mechanical properties with an additional heat treatment of densified material [77].

22

3.10. Mechanical properties

Hydrochar powder was pressed into pellets for mechanical testing. Pelletizing can increase the bulk density and particle size to enable the use of hydrochar as a renewable reducing agent in ferroalloy industries. Hydrochar produced at 230°C was chosen as a feedstock for pelletization due to its low ash and moisture content, high electrical resistance and improved grindability which are comparable with the requirements of ferroalloy industry [78]. Heat treatment of the pellets can further improve their properties, so hydrochar pellets were thermally treated in the range from 250 to 1100°C.
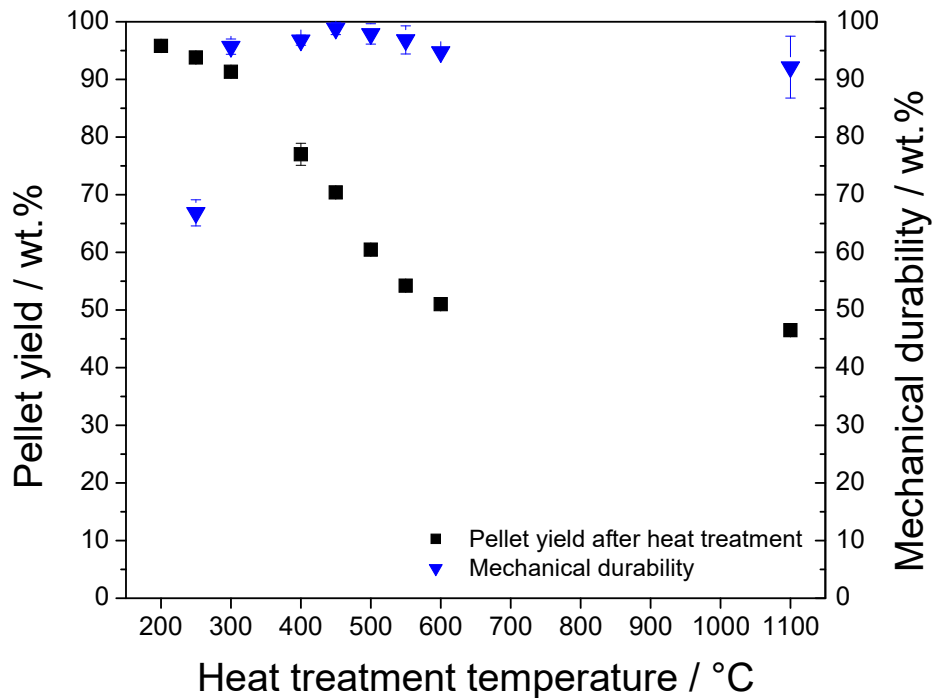

Figure 8: Pellet yield and mechanical durability after heat treatment of hydrochar produced at 230°C with 6 h residence time.

23

The yield and mechanical durability of olive pulp hydrochar pellets after heat treatment are shown in Figure 8. Additional heat treatment and longer residence time during hydrothermal carbonization can result in an increased pellet yield, as summarized in Table 2. Pellets from hydrochar prepared at 200, 220, 230 and 240°C were mechanically stable, confirming the previous results [27, 61, 78]. However, the dried hydrochar pellets without an additional binder were less stable than pellets formed with the addition of water. Previous studies showed that the durability of high quality pellets is required to be $> 97.5\%$ [79]. The additional heat treatment improved the agglomeration of the hydrochar particles, increasing the durability of hydrochar pellets to $> 95\%$ at temperatures above 300°C. A maximum durability of 98.5% was measured during the heat treatment of hydrochar at 450°C showing similar properties to charcoal pellets with the pre-mixed biooil binder [64, 77]. Thus, secondary heat treatment improves the mechanical properties of olive waste hydrochar pellets, making them comparable to those observed for reducing agents obtained from non-renewable resources. Further optimization has promise to produce superior materials from this renewable waste feedstock.

Table 2: Electrical resisitivity of hydrocher pellets after compressed and after heat treatment.

Heat treatment temperature °C	Residence time h^{-1}	Density kg m^{-3}	Electrical resistivity mΩm	Pellet residue wt.%, db
After compression				
200	2	0.94	820±200	
	6	0.98	560±150	
	15	0.99	620±150	
220	2	0.97	680±150	
	6	0.97	580±150	
	15	0.98	480±100	
240	2	1.03	600±200	
	6	0.98	410±100	
	15	0.98	200±50	
After heat treatment at 1100°C				
200	2	0.83	8±3	34.8
	6	0.90	20±5	38.8
	15	0.86	12±3	43.9
220	2	0.98	30±7	37.0
	6	0.97	13±4	44.7
	15	0.93	13±5	49.3
240	2	1.02	6±2	46.1
	6	0.92	12±3	48.5
	15	0.93	11±3	51.1

3.11. Electrical properties

Electrical resistivity is a critical parameter for carbon reducing agents. Accordingly, the electrical resistivity of hydrocar was measured, with the results summarized in Table 2. The electrical resistivity of hydrochar pellets decreased with increasing heat treatment temperature and residence time, consistent with the aforementioned compositional and structural changes that occur during HTC. In addition, the electrical resistivity decreased after drying, resulting in improved electrical properties which were similar to these of an insulator. The electrical resistivity of heat treated hydrochar pellets was in the range 35 to 50 mΩm, similar to that observed for charcoal particles and approaching that of metallurgical coke (≈ 0.01 mΩm) [80]. As with me-

chanical properties, thermal treatment of the raw hydrochar improves their electrical properties.

## 4. Discussion

Figures 1-8 establish that waste biomass has the potential to produce high-quality pelletized bioreductants for the ferroalloy industry. An economical process to produce renewable reducing agents will require simultaneous optimization of yield and properties. Unfortunately, the relationships between HTC conditions and hydrochar yield and properties were complex, making rationale optimization difficult. To guide future efforts, the data provided in Figures 1-8 were re-analyzed to develop structure-property relationships that can be used to guide future optimizations of the process.

Several examples of useful structure-property relationship are shown in Figure 9 and the supplemental material (Figure S-5). Increasing the HTC temperature and residence time decreased the electrical resistivity and increase in calorific value with the increasing carbon and decreasing oxygen content. The heating values of hydrochar were in the range of 24 to 30 MJ kg^{-1} which are similar to those of sub-bituminous coal (24 MJ kg^{-1}) used for heat and power generation [81, 82]. Interestingly, the higher heating value of hydrothermally treated olive pulp was similar to that of torrefied olive stones (28.8 MJ kg^{-1}) at 300°C in a rotary slow pyrolysis reactor [53]. Also, longer torrefaction times and greater heat treatment temperatures led to the improvement of higher heating value of olive stones leading to higher carbon and lower oxygen content.
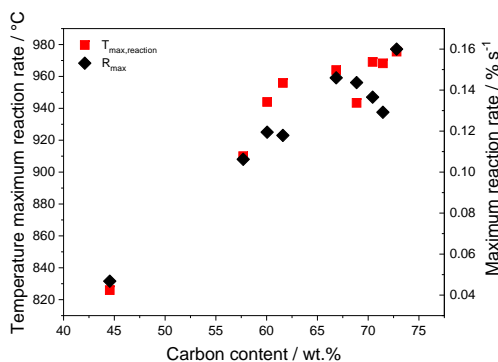
26
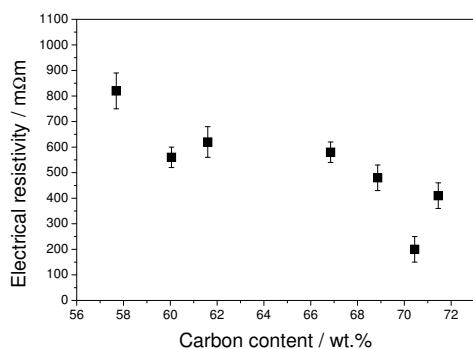
9(a): Electrical resistivity
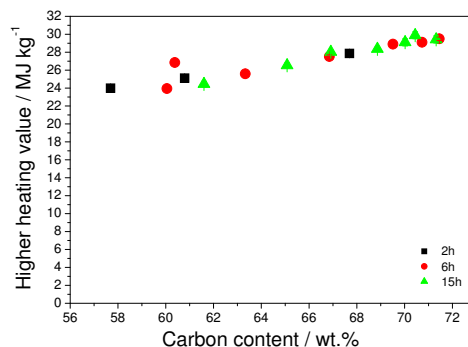
9(b): Higher heating value
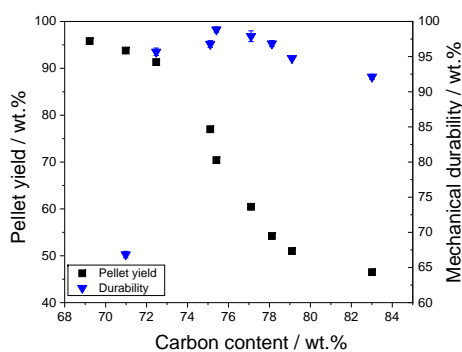
9(c): Pellet yield and mechanical durability

9(d): Reactivity

Figure 9: Correlations of electrical resistivity, higher heating value, pellet yield, mechanical durability, maximum reaction rate and temperature of maximum reaction rate over carbon or oxygen content of hydrochar from olive pulp treatment produced at 190, 220 and 250°C with a residence time of 6 h, olive pulp hydrochar generated at 250°C with a residence time of 6, 15 and 60 h and olive pulp hydrochar prepared at 250°C with a residence time of 6 h further reacted in the range from 300 to 1100°C in a high-temperature furnace.

The electrical resistivity of hydrochars decreased from 800 to 200 mΩm with the increased temperatures and longer residence times. This is due to the decarboxylation reactions leading to the formation of more defects in a

27

molecular structure of hydrochar, confirming the previous results of Hoffmann et al. [83]. Interestingly, the mechanical strength of pellets made from hydrochar decreases slighly from 98 to 92 %, as shown in Figure 9(c). The small differences in mechanical durability of pellets made from hydrochar were related to the small changes in a pellet density. About 50 % of the used water was released during pelletizing, and most of the remaining water was evaporated during storage under atmospheric conditions. The water content of hydrochar pellets after storage in open air containers was approximately 4 wt.%, leading to the improvement of char hydrophobicity due to the removal of -OH groups [61]. The density of hydrochar pellet was 800 kg m^{-3}, and decreased to 760 kg m^{-3} after additional heat treatment at 550°C due to the removal of volatile components and further decomposition of organic matrix [64]. Thus, hydrochar pellets showed a density that is similar to that of spruce charcoal pellets [77]. Interestingly, the density of hydrochar pellets produced from loblolly pine was approximately 50 % greater than that of hydrochar pellets made from olive pulp, indicating the importance of feedstock selection [27, 61]. The density can be increased with pelletization with increased compression force, resulting in improved durability and tensile strength [61, 77]. A compression force of 5 kN resulted in an increased pellet density of approximately 980 kg m^{-3}, suggesting the promise of this method. Pellets obtained from hydrochar prepared at 200 and 250°C showed a negligible swelling (1 %), whereas the remaining water evaporated and an additional decomposition of the hydrochar occurred [84]. The hydrochar pellets shrunk when treated at temperatures greater than used for hydrothermal carbonization resulting in an isotropic shrinkage to about 80 % of its orig-

inal size at 600°C. The shrinkage of hydrochar pellets from olive pulp was similar to that of pellets made from wood and wheat straw, indicating a minor effect of feedstock on the particle shrinkage [84]. The maximum reaction rate of reacted hydrochar samples increased with the higher carbon content, indicating the formation of aromatic and semi-aromatic rings. Crystalline cellulose was nearly completely converted to solid char, whereas the remaining lignin shields the hydrochar and reduces its CO_2 gasification reactivity. The heat treatment temperature and residence time both had an equal influence on the hydrochar aromatization leading to a similar maximum reaction rate when the carbon content was greater than 60 %.

The results of the present work clearly show that the hydrochar properties such electrical resistivity, higher calorific value, durability and reactivity approach the physicochemical properties of metallurgical coke. The major challenge with the use of hydrochar pellets is related to the remaining high oxygen content. Ferroalloy industries require a minimum fixed carbon content of 90 to 95 %, whereas charcoal produced at temperatures between 450 and 550°C obtained fixed carbon content $< 85\%$ [85–87]. Further heat treatment of hydrochar pellets could potentially reduce the oxygen content, enhancing the hydrochar carbon content, as reported in previous studies [88–91]. Mechanochemical treatment may have promise for similar reasons [92]. Additional heat treatment of hydrochar pellets increases the mechanical durability of hydrochar pellets to 99.5 % and density of hydrochar to 980 kg m^{-3}. The high temperature charcoal showed mechanical durability of less than 95 % and with the density of less than 600 kg m^{-3} [64, 65]. High mechanical strength and high density of reductants are desired during

29

transportation and storage of pellets indicating potential of hydrochar use in ferroalloy industries. Overall, the mechanical durability of pellets from hydrotreated olive pulp is greater than that of torrefied olive stones [25]. Therefore, the pretreatment of olive pulp under the suggested hydrotreatment conditions might be more suitable for the production of reductants for the ferroalloy industries than torrefaction.

5. Conclusion

Torrefation and hydrothermal carbonization were investigated for conversion of olive pulp waste to a biorenewable reductant. Fixed carbon yield depends on both heat treatment temperature and residence time in hydrothermal carbonization. Thermo-gravimetric analysis results showed that the CO_2 reactivity of hydrochar is similar to that of olive pulp reacted at 900°C, whereas the effect of heat treatment temperature had less influence on the reactivity with increasing residence time of olive pulp torrefaction. Moreover, hydrocar remained more reactive than fossil-based reductants, such as petroleum coke and metallurgical coke. The hydrochars produced at 220 and 250°C showed a similar surface composition to one another, and similarly residence time had only a minor effect on the char composition. The hydrochar pellets can be densified at low compression pressure without an addition of a binder, whereas a secondary heat treatment at 400°C is required to improve the mechanical durability of hydrochar pellets to satisfy ferroalloy industry requirements. The findings of this study emphasize the potential use of hydrothermal pellets as renewable reducing agents for the ferroalloy industry with future anticipated improvement in hydrochar transportation

and storage.

Acknowledgements

References

[1] Steinfeld A, High-temperature solar thermochemistry for CO_2 mitigation in the extractive metallurgical industry, International Symposium on CO_2 Fixation and Efficient Utilization of Energy (1997).

[2] Balomenos E, Panias D, Paspaliaris I, Energy and exergy analysis of the primary aluminum production processes: A review on current and future sustainability, Min Proc Ext Met Rev 32 (2011) 69–89.

[3] Lu L, Iron Ore: Mineralogy, Processing and Environmental Ssustainability, Elsevier, 2015.

[4] Lu L, Adam M, Kilburn M, Hapugoda S, Somerville M, Jahanshshi S and etc., Substitution of charcoal for coke breeze in iron ore sintering, ISIJ Int 53 (2013) 1607–16.

[5] Matsumura T, Ichida M, Nagasaka T, Kato K, Carbonization behavior of woody biomass and resulting metallurgical coke properties, ISIJ Int 48 (2008) 572–77.

[6] Lovel R, Vining K, Dell'Amico M, Iron ore sintering with charcoal, Miner Process Extr Metal 116 (2007) 85–92.

[7] Macphee JA, Grandsden JF, Giroux L, Price JT, Possible CO_2 mitigation via addition of charcoal to coking coal blends, Fuel Process Technol 90 (2009) 16–20.

[8] Osman AI, Mass spectrometry study of lignocellulosic biomass combustion and pyrolysis with NO_x removal, Renew Energy 146 (2020) 484–96.

[9] Roman S, Libra J, Berge N, Sabio E, Ro K, Li L and etc., Hydrothermal Carbonization: Modeling, Final Properties Design and Applications: A Review, Energies 11 (2018) 1–28.

[10] Tangstad M, Leroy D, Ringdalen E, Behaviour of agglomerates in ferromanganese production, INFACON XII, Hensinki, Finland (2010) 457–66.

[11] Holappa L, Towards sustainability in ferroalloy production, J South African Inst Min Metal 110 (2010) 1–8.

[12] Bullock C, Hawe J, Little D, Realising the ecosystem-service value of native woodland in Ireland, New Zeal J Forest Sci 44 (2014) 1–10.

[13] Pardo de Donlebun JPA, The EU enlargement in 2004: analysis of the forestry situation and perspectives in relation to the present EU and Sweden. Skogsstyrelsen National Board of Forestry. Jönköping: Sweden; 2003 October Report No. ISSN1100-0295 (????).

[14] de Jong J, Akselsson C, Berglund H, Egnell G, Gerhardt K, Lönnberg L and etc., Consequences of an increased extraction of forest biofuel in Sweden. Swedish Energy Agency. Eskilstuna: Sweden; 2014 September Report No. ISSN1403-1892 (????).

[15] Pawelczyk A, EU policy and legislation on recycling of organic wastes to agriculture, ISAH 1 (2005) 64–71.

[16] Ouazzane H, Laajine F, El Yamani M, El Hilaly J, Rharrabti Y, Amarouch MY and et al., Olive Mill Solid Waste Characterization and Recycling Opportunities: A review, JMES 8 (2017) 2632–50.

[17] Benavente V, Fullana A, Torrefaction of olive mill waste, Biomass Bioenergy 73 (2015) 186–94.

[18] Pistorius PC, Reductant selection in ferro-alloy production: The case for the importance of dissolution in the metal, J South African Inst Min Met 1 (2002) 33–6.

[19] Sahajwalla V, Dubikova M, Khanna R, Reductant characterisation and selection: implications for ferroalloys processing, 10th Int Ferroalloys Congress INFACON X. Transformation through Technology 68 (2004) 351–62.

[20] Wang L, Zhang Z, Qu Y, Guo Y, Wang Z, Wang X, A novel route for preparation of high-performance porous carbons from hydrochars by KOH activation, Colloids Surf A Physicochem Eng Asp 447 (2014) 183–7.

[21] Unur E, Brutti S, Panero S, Scrosati B, Nanoporous carbons from hydrothermally treated biomass as anode materials for lithium ion batteries, Micropor Mesopor Mater 174 (2013) 25–33.

[22] Hitzl M, Corma A, Pomares F, Renz M, The hydrothermal carbonization (HTC) plant as adecentral biorefinery for wet biomass, Catal Today 257 (2015) 154–9.

34

[23] Funke A, Reebs F, Kruse A, Experimental comparison of hydrothermal and vapothermal carbonization, Fuel Proc Tech 115 (2013) 261–9.

[24] Ahmad F, Silva EL, Varesche MBA, Hydrothermal processing of biomass for anaerobic digestion - A review, Renew Sust Energ Rev 98 (2018) 108–24.

[25] Trubetskaya A, Leahy JJ, Müller M, Layden P, Johnson R, Stahl K, Yazhenskikh E, Monaghan RFD, Characterization of woodstove briquettes from torrefied biomass and coal, Energy 171 (2019) 853–65.

[26] Kambo HS, Dutta A, A comparative review of biochar and hydrochar in terms of production, physico-chemical properties and applications, Renew Sust Energy Rev 45 (2015) 359–78.

[27] He C, Tang C, Li C, Yuan J, Tran KQ, Bach QV and et al., Wet torrefaction of biomass for high quality solid fuel production: A review, Renew Sust Energ Rev 91 (2018) 259–71.

[28] Smith A, Singh S, Ross A, Fate of inorganic material during hydrothermal carbonisation of biomass: Influence of feedstock on combustion behavior of hydrochar, Fuel 169 (2016) 135–45.

[29] Trubetskaya A, Jensen PA, Jensen AD, Steibel M, Spliethoff H, Glarborg P, Influence of fast pyrolysis conditions on yield and structural transformation of biomass chars, Fuel Proc Tech 140 (2016) 205–13.

[30] Hardi F, Imai A, Theppitak S, Kirtania K, Furusjö E, Yoshikawa K, Gasification of Char Derived from Catalytic Hydrothermal Liquefaction

of Pine Sawdust under a CO_2 Atmosphere, Energy Fuels 32 (2018) 5999–6007.

[31] Reza MT, Lynam JG, Uddin MH, Coronella CJ, Hydrothermal carbonization: Facte of inorganics, Energy Procedia 49 (2013) 86–94.

[32] Mosqueda A, Medrano K, Gonzales H, Yoshikawa K, Effect of hydrothermal and washing treatment of banana leaves on co-gasification reactivity with coal, Energy Procedia 158 (2019) 785–91.

[33] Cai J, Li B, Chen C, Wang J, Zhao M, Zhang K, Hydrothermal carbonization of tobacco stalk for fuel application, Biores Tech 220 (2016) 305–11.

[34] Novianti S, Nurdiawati A, Zaini IN, Prawisudha P, Sumida H, Yoshikawa K, Low-potassium Fuel Production from Empty Fruit Bunches by Hydrothermal Treatment Processing and Water Leaching, Energy Procedia 75 (2015) 584–9.

[35] Yamagishi K, Endo K, Saga J, A comprehensive analysis of the furnace interior for high-carbon ferrochromium, 1th Int Ferroalloys Congress INFACON 74. Transformation through Technology (1974) 143–7.

[36] De Waal A, Barker IJ, Rennie MS, Klopper J, Groeneveld BS, Electrical Factors Affecting the Economic Optimization of Submerged-arc Furnaces, 6th Int Ferroalloys Congress INFACON 6. Transformation through Technology 1 (1974) 247–52.

[37] Strandberg A, Thyrel M, Skoglund N, Lestander TA, Broström M, Backman R, Biomass pellet combustion: Cavities and ash formation charac-

609 terized by synchrotron X-ray microtomography, Fuel Process Tech 176
610 (2018) 211–20.

611 [38] Shang L, Ahrenfeldt J, Holm JK, Sanadi AR, Talbro Barsberg S, Thom-
612 sen T and etc., Changes of chemical and mechanical behavior of torrefied
613 wheat straw, Biomass Bioenergy 40 (2012) 63–70.

614 [39] Li T, Geier MT, Wang L, Shaddix CR, Ku X, Matas Güell B and etc.,
615 Effect of Torrefaction on Physical Properties and Conversion Behavior
616 of High Heating Rate Char of Forest Residue, Energy Fuels 29 (2015)
617 177–84.

618 [40] Bajcar M, Zagula G, Saletnik B, Tarapatskyy M, Puchalski C, Relation-
619 ship between Torrefaction Parameters and Physicochemical Properties
620 of Torrefied Products Obtained from Selected Plant Biomass, Energies
621 11 (2018) 1–13.

622 [41] Shoulaifar TK, DeMartini N, Zevenhoven M, Verhoeff F, Kiel J, Hupa
623 M, Ash-Forming Matter in Torrefied Birch Wood: Changes in Chemical
624 Association, Energy Fuels 27 (2013) 5684–90.

625 [42] Medic C, Darr M, Shah A, Potter B, Zimmermann J, Effects of tor-
626 refaction process parameters on biomass feedstock upgrading, Fuel 91
627 (2012) 147–54.

628 [43] Volpe M, Fiori L, From olive waste to solid biofuel through hydrothermal
629 carbonization: The role of temperature and solid load on secondary
630 char formation and hydrochar energy properties, J Anal Appl Pyrol 124
631 (2017) 63–72.

37

[44] Liu Z, Quek A, Balasubramanian R, Preparation and characterization of fuel pellets from woody biomass, agro-residues and their corresponding hydrochars, Appl Energy 113 (2014) 1315–22.

[45] Lucian M, Fiori L, Hydrothermal carbonization of waste biomass: Process design, modeling, energy efficiency and cost analysis, Energies 10 (2017).

[46] Mandova H, Leduc S, Wang C, Wetterlund E, Patrizio P, Kraxner F and etc., Possibilities for CO_2 emission reduction using biomass in European integrated steel plants, Biomass Bioenergy 115 (2018) 231–43.

[47] Saba A, McGauphy K, Reza MT, Techno-Economic Assessment of Co-hydrothermal carbonization of a Coal-Miscanthus Blend, Energies 12 (2019) 1–17.

[48] Surup GR, Nielsen HK, Attard TM, Trubetskaya A, Hunt AJ, Arshadi M and etc., The effect of wood composition and supercritical CO_2 extraction on charcoal production in ferroalloy industries, Energy 193 (2020) 116696.

[49] Van Wesenbeeck S, Wang L, Ronsse F, Prins W, Skreiberg Ø, Antal MJ, Charcoal "mines" in Norwegian Woods, Energy Fuels 30 (2016).

[50] Mazumder B, Chapter 4. Analysis of Coal. In: Coal Science and Engineering, WPI, 2012.

[51] Sun L, Wang J, Bonaccurso E, Conductivity of individual particles measured by a microscopic four-point-probe method, Sci Rep 3 (2013) 1–5.

[52] L. van der Pauw, A Method of Measuring Specific Resistivity and Hall Effect of Discs of Arbitrary Shape, Philips Res Rep 13 (1958) 1–9.

[53] Sangines P, Dominguez MP, Sanchez F, San Miguel G, Slow pyrolysis of olive stones in a rotary kiln: Chemical and energy characterization of solid, gas, and condensable products, J Ren Sust Energy 7 (2015) 1–13.

[54] Stirling RJ, Snape CE, Meredith W, The impact of hydrothermal carbonization on the char reactivity of biomass, Fuel Process Technol 177 (2018) 152–8.

[55] Missaoui A, Bostyn S, Belandria V, Cagnon B, Sarh B, Gökalp I, Hydrothermal carbonization of dried olive pomace: Energy potential and process performances, J Anal Appl Pyrol 128 (2017) 281–90.

[56] Zhang L, Liu S, Wang B, Wang Q, Yang G, Chen J, Effect of Residence Time on Hydrothermal Carbonization of Corn Cob Residual, Bioresources 10 (2015) 3979–86.

[57] Uddin MH, Reza MT, Lynam JG, Coronella CJ, Effects of Water Recycling in Hydrothermal Carbonization of Loblolly Pine, Environ Prog Sustain 33 (2014) 1309–15.

[58] Stemann J, Ziegler F, Hydrothermal Carbonisation (HTC): Recycling of Process Water, $19^{t}h$ EUBCE (2011) 1894–9.

[59] Guo S, Dong X, Liu K, Yu H, Zhu C, Chemical, energetic, and structural characteristics of hydrothermal carbonization solid products for lawn grass, BioRes 10 (2015) 4613–25.

[60] Yang B, Gray MC, Liu C, Lloyd TA, Stuhler SL, Wyman CE, et al., Unconventional Relationships for Hemicellulose Hydrolysis and Subsequent Cellulose Digestion., Lignocellulose Biodegradation (2004) 100–25.

[61] Bach QV, Skreiberg Ø, Upgrading biomass fuels via wet torrefaction: A review and comparison with dry torrefaction, Renew Sust Energ Rev 54 (2016) 665–77.

[62] Dinjus E, Kruse A, Tröger N, Hydrothermal Carbonization - 1. Influence of Lignin in Lignocelluloses, Chem Eng Technol 34 (2011) 2037–43.

[63] Liu Z, Quek A, Hoekman SK, Balasubramanian R, Production of solid biochar fuel from waste biomass by hydrothermal carbonization, Fuel 103 (2013) 943–9.

[64] Surup GR, Vehus T, Eidem PA, Trubetskaya A, Nielsen HK, Characterization of renewable reductants and charcoal-based pellets for the use in ferroalloy industries, Energy 167 (2019) 337–45.

[65] Surup GR, Nielsen HK, Heidelmann M, Trubetskaya A, Characterization and reactivity of charcoal from high temperature pyrolysis (800–1600°C), Fuel 235 (2019) 1544–54.

[66] Titirici MM, Thomas A, Yu SH, Müller JO, Antonietti M, A Direct Synthesis of Mesoporous Carbons with Bicontinuous Pore Morphology from Crude Plant Material by Hydrothermal Carbonization, Chem Mater 19 (2007) 4205–12.

[67] Hansen TL, Schmidt JE, Angelidaki I, Marca E, la Cour Jansen J, Christensen TH, et al., Method for determination of methane potentials of solid organic waste, Waste Management 24 (2004) 393–400.

[68] Kobayashi F, Take H, Asada C, Nakamura Y, Methane production from steam-exploded bamboo, J Biosci Bioeng 97 (2004) 426–8.

[69] Mumme J, Eckervogt L, Pielert J, Diakité M, Rupp F, Kern J, Hydrothermal carbonization of anaerobically digested maize silage, Biores Tech 102 (2011) 9255–60.

[70] Arellano O, Flores M, Guerra J, Hidalgo A, Rojas D, Strubinger A, Hydrothermal Carbonization of Corncob and Characterization of the Obtained Hydrochar, Chem Eng Trans 50 (2016) 235–40.

[71] El-Hendawy ANA, Variation in the FTIR spectra of a biomass under impregnation, carbonization and oxidation conditions, J Anal Appl Pyrolysis 75 (2004) 159–66.

[72] Fan M, Dai D, Huang B, Chapter 3 Fourier Transform Infrared Spectroscopy for Natural Fibres. In (ed. Salih SM): Fourier Transform, IntechOpen (2012) 45–68.

[73] Adapa PK, Tabil LG, Schoenau GJ, Canam T, Dumonceaux T, Quantitative Analysis of Lignocellulosic Components of Non-Treated and Steam Exploded Barley, Canola, Oat and Wheat Straw Using Fourier Transform Infrared Spectroscopy, J Agr Sci Tech B 1 (2011) 177–88.

[74] Arafat A, Samad SA, Masum SM, Moniruzzaman M, Preparation and

720 Characterization of Chitosan from Shrimp shell waste, IJSER 6 (2015) 721 538–41.

[75] Labbé N, Harper D, Rials T, Elder T, Chemical Structure of Wood Charcoal by Infrared Spectroscopy and Multivariate Analysis, J Agr Food Chem 54 (2006) 3492–7.

[76] Viswanathan B, Coal, Energy Sources (2017) 81–111.

[77] Riva L, Surup GR, Buø TV, Nielsen HK, A study of densified biochar as carbon source in the silicon and ferrosilicon production, Energy 181 (2019) 985–96.

[78] Wnukowski M, Owczarek P, Niedźwiecki Ł, Wet torrefaction of miscanthus - Characterization of hydrochars in view of handling, storage and combustion properties, J Ecol Eng 16 (2015) 161–7.

[79] Abedi A, Cheng H, Dalai AK, Effects of natural additives on the properties of sawdust fuel pellets, Energy Fuels 32 (2018) 1863–73.

[80] Eidem PA, Tangstad M, Bakken JA, Determination of Electrical Resistivity of Dry Coke Beds, Metallurgical and Materials Transactions B 39 (2008) 7–15.

[81] Basu P, Biomass Gasification and Pyrolysis: Practical Design and Theory, Elsevier, 2010.

[82] Tumuluru JS, Hess JR, Boardman RD, Wright CT, Westover TL, Formulation, Pretreatment, and Densification Options to Improve Biomass

741 Specifications for Co-Firing High Percentages with Coal, Ind Biotech 8
742 (2012) 113–32.

[83] Hoffmann V, Jung D, Zimmermann J, Rodriquez Correa C, Elleuch
A, Halouani K and etc., Conductive Carbon Materials from the Hy-
drothermal Carbonization of Vineyard Residues for the Application in
Electrochemical Double-Layer Capacitors (EDLCs) and Direct Carbon
Fuel Cells (DCFCs), Materials 12 (2019) 1–33.

[84] Paulauskas R, Striugas N, Zakarauskas K, Dziugys A, Vorotinskiene L,
Investigations of regularities of pelletized biomass thermal deformations
during pyrolysis, Therm Sci 22 (2018) 603–12.

[85] Oliveira FR, Patel AK, Jaisi DP, Adhikari S, Lu H, Environmental
application of biochar: Current status and perspectives, Biores Tech
246 (2017) 110–22.

[86] Tan Z, Lin CSK, Ji X, Rainey TJ, Returning biochar to fields: A review,
Appl Soil Ecol 116 (2017) 1–11.

[87] Tripathi M, Sahu JN, Ganesan P, Effect of process parameters on pro-
duction of biochar from biomass waste through pyrolysis: A review,
Renew Sust Energy Rev 55 (2016) 467–81.

[88] M. Díez, R. Alvarez, C. Barriocanal, Coal for metallurgical coke pro-
duction: Predictions of coke quality and future requirements for coke-
making, INT J COAL GEOL 50 (2002) 389–412.

[89] A. Babich, D. Senk, Chapter 12 - coal use in iron and steel metallurgy,

763   in: D. Osborne (Ed.), The Coal Handbook: Towards Cleaner Produc-
764   tion, volume 2 of *Woodhead Publishing Series in Energy*, Woodhead
765   Publishing, 2013, pp. 267–311.

766 [90] H. Schobert, N. Schobert, Comparative carbon footprints of metallur-
767   gical coke and anthracite for blast furnace and electric arc furnace use,
768   2015.

769 [91] United States International Trade Commission, Metallurgical Coke:
770   Baseline Analysis of the U.S. Industry and Imports : [investigation No.
771   332-342]., USITC publication, U.S. International Trade Commission,
772   1994.

773 [92] Timko MT, Maag AR, Venegas JMand McKeogh B, Yang Z, Escapa
774   S and etc., Spectroscopic tracking of mechanochemical reactivity and
775   modification of a hydrothermal char, RSC advances 6 (2016).